ADVANCED MATERIALS TECHNOLOGIES
www.advmattechnol.de

Core–Sheath Stretchable Conductive Fibers for Safe Underwater Wearable Electronics

*Yan Zhang, Weifeng Zhang, Guo Ye, Qishuo Tan, Yan Zhao, Jiakang Qiu, Shuyan Qi, Xiaojia Du, Tinglei Chen, and Nan Liu**

Stretchable conductive fibers can be directly woven into textiles and applied in wearable and implantable electronic devices. However, for a stretchable conductive fiber that is capable of safely using in full water environment with strains when contacting to skin, it is challenging. Herein, an ultrafine core–sheath stretchable conductive fiber (CSCF in short) with insulative outer sheath and conductive inner core is designed particularly for safe underwater electronic skin devices. CSCF starts from prestrained Lycra fiber followed by spray coating 1D conductive species (carbon nanotubes (CNTs)/silver nanowires (AgNWs)) and wrapping styrene-(ethylene-butylene)-styrene (SEBS) thin film. CSCF exhibits stable core conductivity (e.g., $R_0 \approx 2 \times 10^4$ S m^{-1}, $\Delta R/R_0 \approx 0.1$ at 100% strain) as well as surface insulation upon mechanical stretching in full water environment. The thickness-tunable SEBS not only protects skin away from leak of CNTs and AgNWs, but also efficiently suppresses leakage current to an extremely safe level (<1 μA at 5 V) when applying in underwater electronic skin devices. A wireless charging patch composed by CSCF induction coil is able to light light emitting diode (LEDs) no matter when CSCFs are folding and stretching in water. These advantages highlight the promising application of stretchable conductive fiber with protective polymer skin for safe underwater wearable electronics.

Wearable electronics refers to smart electronic devices that can be worn on the body as accessories or implants, including physiological monitors, biomedical sensors, energy conversions and storage, wireless communication and charging systems, and human–machine interactors.[1–8] They are highly desired to be conformable to enable good signal quality during the movement of the wearer and to be lightweight and long-lasting. Incorporating electrically-functional fibers into textiles is a convenient method to impart sensing and readout functionality in the form of wearable clothing. Developing these smart electronic textiles (E-textiles) requires stretchable conductive fibers with high electrical conductivity and mechanical durability to enable textiles that are washable with lifetimes similar to conventional textiles.[9–13] Furthermore, our daily life cannot be without water, such as raining, bathing, swimming, and etc. With underwater wearable electronics, underwater activities can be effectively detected or analyzed, for example monitoring electrophysiological signals for athletes when they are training in the rain or water, detecting the moving, migration or feeling of the living creatures underwater. Therefore, to design stretchable conductive fibers capable of working in full water environment is fundamentally essential. Typical methods of developing stretchable conductive fibers include prestraining polymer fibers to induce the attached 1D conductive species (metal nanowires or carbon nanotubes (CNTs)) into wavy structure,[3,14] wrapping conductive species into spiral shape along an elastic polymer fiber,[3,10,15–19] or using a conductive liquid or gel encapsulated in an elastomer.[20–22] However, liquid metal conductors are susceptible to leakage if the fibers are damaged, while hydrogel conductors dry out over time, and both exhibit changes in conductance of the fibers with strain. Carbon-based conductors have low conductivity with increasing length,[7,9,14,17,23,24] while metal composite conductors typically exhibit limited strain tolerance and poor cycle stability.[25,26] Conductive fibers with waterproof[27] or splash-resistance[28] have been studied, but stretchable conductive fibers that are capable of maintaining good conductivity at high strain as well as fully underwater long-time use have not been systematically reported yet.

In this work, we presented a core–sheath stretchable conductive fiber (CSCF) which could be safely used in water and other harsh environments (such as sonication) for a long time. The ultrafine CSCF (≈30 μm in diameter) is composed of Lycra (polyurethane, PU) fiber, multiwall carbon nanotubes (MWCNTs), silver nanowires (AgNWs), and styrene-(ethylene-butylene)-styrene (SEBS) sequentially from inside to outside, which is defined as PU@CNTs@AgNWs@SEBS. Spray coating 1D conductive networks onto a prestraining Lycra fiber resulted in a highly stretchable conductive fiber (e.g., $\Delta R/R_0 \approx 0.1$ at 100% strain, cycled >100 000 times at 50% strain). Surface coating SEBS enabled a significantly reduced leakage both in current (<1 μA at 5 V) and element (Ag), thus safe to human

Y. Zhang, W. Zhang, G. Ye, Q. Tan, Y. Zhao, J. Qiu, S. Qi, X. Du, T. Chen, Prof. N. Liu
Beijing Key Laboratory of Energy Conversion and Storage Materials
College of Chemistry
Beijing Normal University
Beijing 100875, P. R. China
E-mail: nanliu@bnu.edu.cn

The ORCID identification number(s) for the author(s) of this article can be found under https://doi.org/10.1002/admt.201900880.

DOI: 10.1002/admt.201900880

body (<0.5–1 mA).[29] With this elastic and reliable protective SEBS skin, CSCF can be circled as a stretchable inductance coil and work as a wireless charging patch in water. This implies that our CSCF is promising as stretchable connector or electrode for underwater wearable electronics.

To develop underwater wearable electronics, conductive fibers having stable electrical performance under deformation and being safe to living creatures in water are two prerequisites. Safety mainly refers to material biocompatibility as well as a safe current sensed by the creatures. **Figure 1**a presents a core–sheath stretchable conductive fiber (CSCF), particularly designed for underwater wearable electronics. Commercialized Lycra fiber (≈30 µm in diameter) is used as the core of CSCF. The main composition of Lycra is PU which has been widely applied in the textile industry for manufacturing elastic fibers and fabrics.[30,31] Because PU is made by the exothermic reactions between alcohols and isocyanates, it can easily react with carboxyl or hydroxyl groups forming hydrogen bonds. CNTs produced by catalytic chemical vapor deposition method inevitably contain oxygen-containing functional groups. Therefore, when spray coating MWCNTs, they can adhere onto the sidewall of PU very well, but AgNWs are not coated well (Figure S1, Supporting Information). Thus, MWCNTs are chosen as the first conductive layer that has good electronic injection capacity. Following MWCNTs, AgNWs as current collector were applied to further enhance their conductivity (up to ≈2×10^4 S m^{-1}). The outermost material is SEBS, which aims to offer the safe property to CSCF including biocompatibility and electrical insulation to human skin. To enable the core–sheath fibers to be stretchable conductive fibers, hierarchically buckling method was applied.[14,32,33] Figure 1b presents the fabrication process of CSCF. First, PU was prestretched to a certain degree with two ends fixed. Then, MWCNTs, AgNWs, and SEBS were spray coated sequentially onto PU by airbrush under compressive nitrogen. After SEBS cured, the fiber was released to its original length along with wrinkle formation. We hypothesized that thus-fabricated fiber could be a stretchable conductive fiber, as it is made by hierarchically buckling method with a series of materials PU@CNTs@AgNWs@SEBS.

Center of **Figure 2**a shows the schematic of CSCF in longitudinal section view, which is composed of elastic PU core (light green), conductive layers (MWCNTs in black, AgNWs in purple) and SEBS elastic skin (green). Outermost surface and inner layers of thus-fabricated fiber are shown in the scanning electron microscope (SEM) images on the left and right (top: AgNWs; bottom: MWCNTs) of Figure 2a respectively. Periodic hierarchical buckling along the fiber axis was observed and their densities are proportional to the applied prestrain along the longitudinal axis of PU. As illustrated in Figure S2 in the Supporting Information, higher degree of prestrain leads to larger wrinkle density at the surface of the fiber. Reversibly, while stretching the fibers, wrinkles can be gradually released (Figure 2b). Thus, this hierarchical buckling imparts the fiber a stronger capability to release strain, potentially showing a more stable conductivity at strain.[14,32,33] In all these scenarios during release and stretch processes, no single carbon nanotube or AgNW was found at the surface of the fiber in SEM. Moreover, energy dispersive spectroscopy (EDS) mapping over this fiber did not detect Ag signal either (Figure S3, Supporting

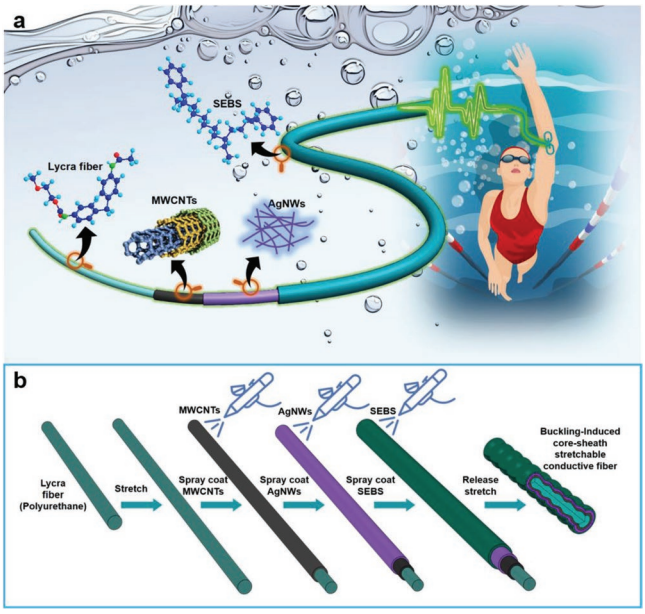

Figure 1. Schematics for core–sheath stretchable conductive fiber (CSCF) for underwater wearable electronics. a) The structure of CSCF. b) The fabrication process of CSCF.

Information). These indicate that thermoplastic SEBS elastomer can wrap up the underlying conductive AgNWs and MWCNTs layers very well. In contrast, other polymers, such as thermoplastic PU and polyvinyl alcohol (PVA), and thermosetting polydimethylsiloxane (PDMS) exhibited poor wetting behaviors with the underlying conductive layers, which are hard to form smooth and thin conductive fiber. Therefore, PU elastic core and SEBS elastic skin, together with MWCNTs and AgNWs as adhesive and conductive layers in between are chosen to make this core–sheath stretchable fiber. The diameter of thus-fabricated fiber is 30 µm in average, which is even thinner than hair (Figure 2c). This ultrafine fiber is an excellent candidate for light-weight wearable electronic devices.

To obtain stretchable conductive fiber, 1D conductive networks were spray coated onto the surface of elastic PU which was prestretched at various prestrains. **Figure 3**a compares the strain dependences of resistance change of core–sheath conductive fibers formed at different prestrains. The core–sheath fibers with prestrains showed obviously stable conductivity than that without prestrain upon stretching. Figure 3b is zoom-in plots of Figure 3a circled in rectangle. The larger the prestrain, the more stable conductivity is thus formed in core–sheath fiber at a certain strain. This could be attributed to the higher wrinkle density induced by larger prestrain. Considering the mechanical property of Lycra fiber, single Lycra fiber will tend to be broken over 300% strain. Thus, 300% prestrain was an optimized parameter and without further specification, our CSCF is formed at this prestrain. As shown in Figure 3c, CSCF exhibited a superior stable core conductivity upon stretching ($\Delta R/R_0 \approx 0.1$ at 100% strain) which is among the best overall performance of stretchable conductive fiber reported so far (Figure 3f).[11,28,31,34–36] The fatigue resistance is also key to the cyclic use for wearable electronics. The fatigue lifetime of CSCF at cyclic strain of 50% was tested in Figure 3d. Core–sheath fibers formed

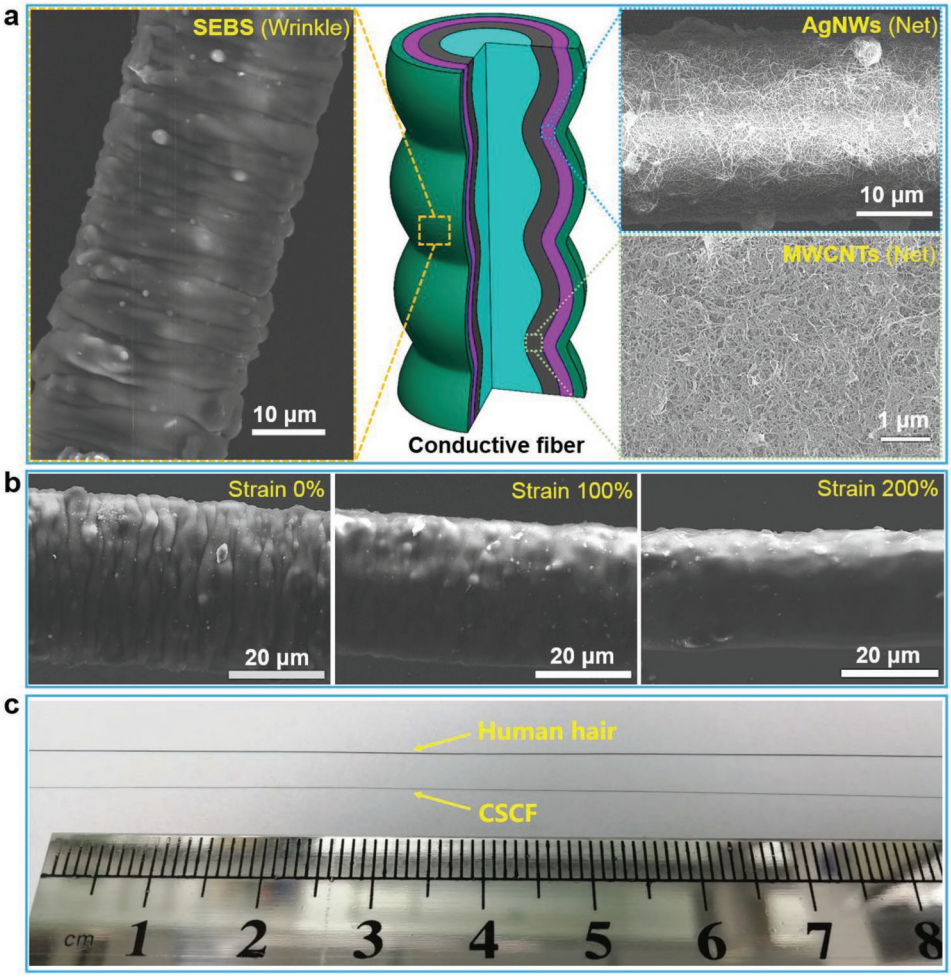

Figure 2. The structure and surface morphology of CSCF. a) Longitudinal section structure of CSCF (center); SEM images of wrinkled outermost surface (left) and inner layers of AgNWs (top right) and MWCNTs (bottom right). b) SEM images of a typical CSCF stretching at different strains, showing different wrinkle-released degrees. c) Photos of an individual CSCF (bottom) and an obviously thinner human hair (top).

with prestrains had much better fatigue resistance than that without prestrain, because energy from cyclic stress could be dissipated by wrinkles. While after cycling over 50 000 times, conductivity of those fibers without prestrain also tends to be stable, possibly due to the adaption of destructive conductive paths.[37,38] Cyclic number of core–sheath fibers with prestrain in the range of 100–300% could reach up to 100 000, where no significant changes in conductivity were found. When people are exercising, the corresponding tensile strain of human skin is just about 3–55%,[10,39] indicating that our CSCF is extremely qualified in wearable electronics regarding its electrical stability. In addition, capability of withstanding repeated washing was tested. Resistance change was monitored when CSCF was immersed in water with magnetic stirring at 600 rpm (rotation per minute) (Figure 3e, details in Note S1 and Figure S4 in the Supporting Information). After 10 washing cycles, there was no significant change in resistance of CSCF, confirming the practicability of CSCF in underwater wearable electronics.

In addition to electrical stability, another characteristic of conductive fiber required in wearable electronic devices is safety. We applied a thin SEBS skin in our CSCF to solve this problem. First, to confirm the protective effect of SEBS skin under water, their resistance changes were monitored along with sonication (**Figure 4**a). In contrast to core–sheath fiber without SEBS, CSCF exhibited stable conductivity during sonication. Next, EDS equipped in SEM was analyzed on CSCF before and after water-bath sonication at a power of 300 W and frequency of 40 kHz. No Ag signal was detected in both cases (after: Figure 4b, before: Figure S3, Supporting Information). Both of elemental analysis and electrical test verify that such biologically compatible SEBS layer is able to prevent the outlets of Ag, which could be a potential toxic source of CSCF.[40–42] In terms of underwater E-textile, such as swimming suits and wearable patches, the cyclic use in water and air is highly possible. Protective effect of SEBS layer when CSCF is cyclically used between water and air was next investigated. As shown in Figure S5 in the Supporting Information, conductivities of core–sheath fibers at 50% strain soaking in water and then fully dried in air were tested respectively. The periodic testes were repeated for 50 times. Comparing the two pairs of conductivity, $\Delta R/R_0$ (%) of CSCF is as small as 1.6% after cyclic tests between water and air for 50 times, while that of fiber without SEBS reached to

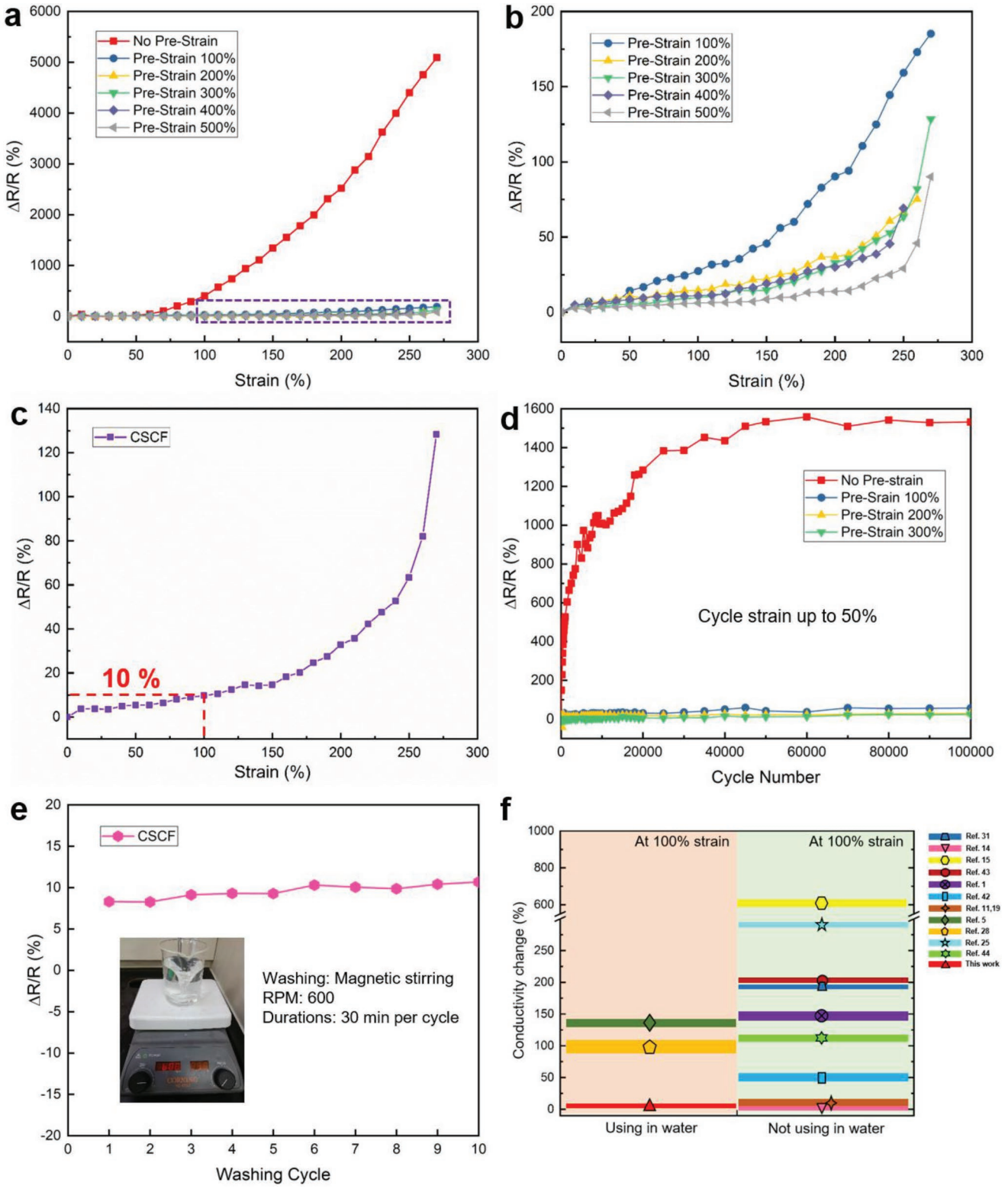

Figure 3. The strain dependence of conductivity for core–sheath fibers. a) Resistance change versus strain of core–sheath fibers formed at different prestrains. b) Zoom-in plots of the rectangular region in (a). c) Resistance change versus strain of a representative CSCF. a–c) Strain rate: 5% s^{-1}. d) Fatigue tests measured the resistance change of core–sheath fibers formed at different prestrains cycled up to 50% strain for 100 000 times. Strain rate: 100% s^{-1}. e) Resistance change of CSCF versus washing cycles in water under magnetic stirring. f) Comparison of CSCF with some other reported works. CSCF exhibits a better overall performance in terms of mechanical electrostability and underwater behavior.

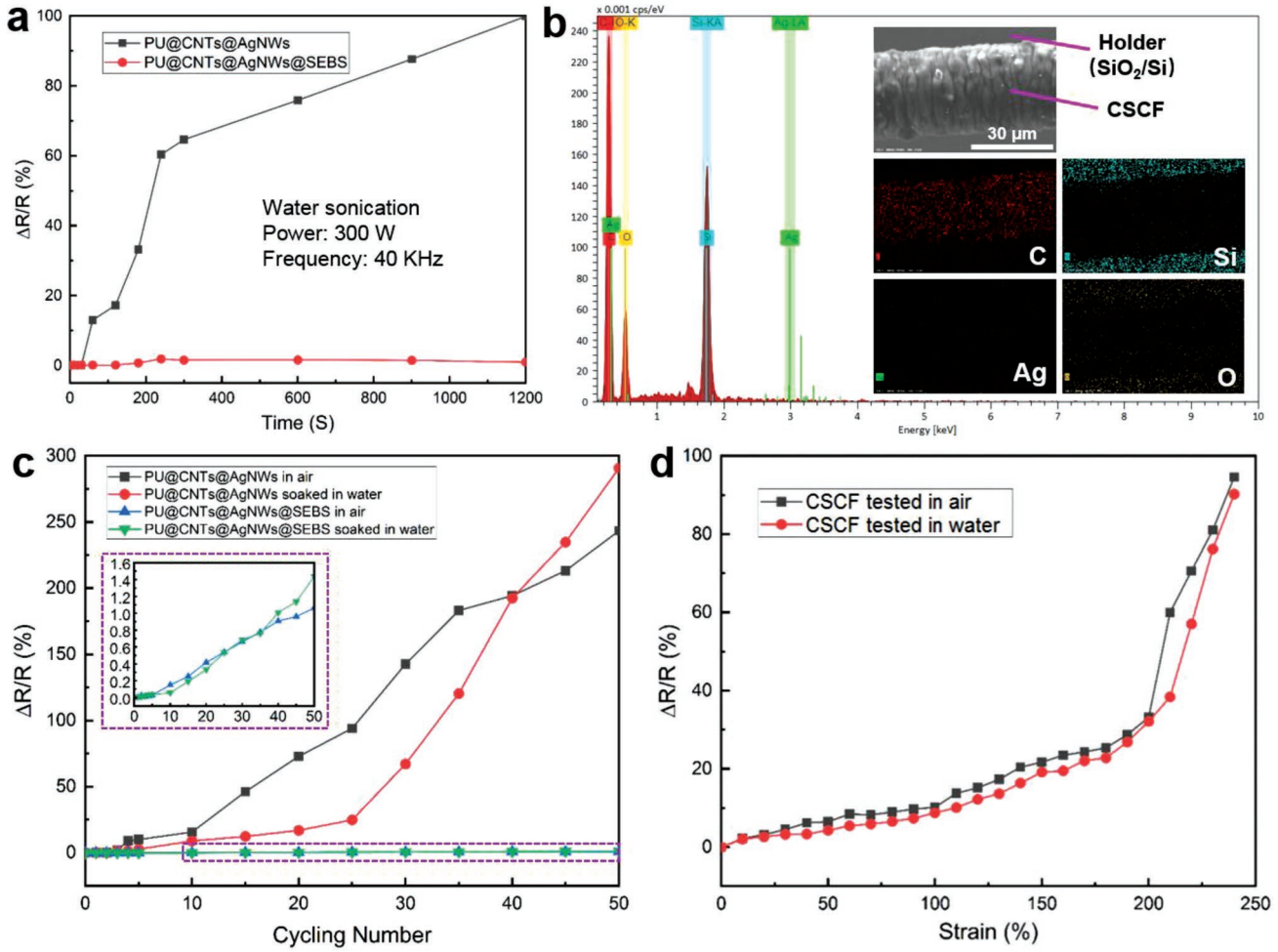

Figure 4. Materials-insulation effect of SEBS layer on CSCF under various circumstances. a) Monitoring resistance change of core–sheath fibers with and without SEBS after water sonication. b) EDS analysis at the surface of CSCF after water sonication at 300 W and 40 kHz for 1 h, showing no leak of Ag. c) Cyclic use of fibers at 50% strain in water and air. Resistance change of core–sheath fibers with and without SEBS alternatively tested in water and in air after water soaking. Inset is zoom-in plots of the rectangular region. d) Resistance change versus strain of CSCF tested in air and water. Strain rate: 5% s^{-1}.

300% (Figure 4c). This again confirms that SEBS skin prevents the detachment of conductive species under water. On the other hand, this additional SEBS layer does make CSCF insensitive to water under strain, showing almost identical resistance changes versus strain in both in air and water (Figure 4d). These results suggest that with the protection of SEBS skin, our CSCF can be long used in water even under harsh environment.

SEBS also plays the role of a conductivity–insulation layer. When approaching or contacting CSCF onto human skin, SEBS prohibits leakage current and possibly toxic materials or elements from inner CSCF to human skin. As shown in **Figure 5**a, a circuit model was summarized on the leakage current sensed by skin in water when CSCF is connected in series with supply power. The current between possibly existed micro holes (red points) on CSCF and human skin is the leakage current, calculated in the following equation

$$I_L = U\sum_{i=1}^{n} \frac{R_i C_i}{R_i + C_i} \quad (1)$$

Herein, I_L is leakage current, U is voltage applied on the CSCF, R_i is point resistance, C_i is point capacitance and n is the point number. To simplify this model, we used Ag/AgCl as counter electrode to mimic skin, and measured the current between core–sheath fiber and Ag/AgCl as leakage current in water (Figure 5b, Figure S6, Supporting Information), which is referenced to leakage current measurement method in transistor.[43,44] Because normally electronic device is driven below 5 V, applied voltage (U) is set in the range of 0–5 V. Figure 5c,d compared the leakage current versus applied voltage on core–sheath fibers in same length without and with SEBS at different distances between fiber and Ag/AgCl electrode. According to Equation (1), maximum leakage current will be occurred when CSCF directly contacts with skin. Therefore, the leakage current in direct contact between CSCF and skin is focused. In Figure 5c, when fiber without SEBS insulation layer directly contacts with skin at voltage of 5 V, leakage current reaches to 2 mA which is higher than 0.5–1 mA the maximum safety current that

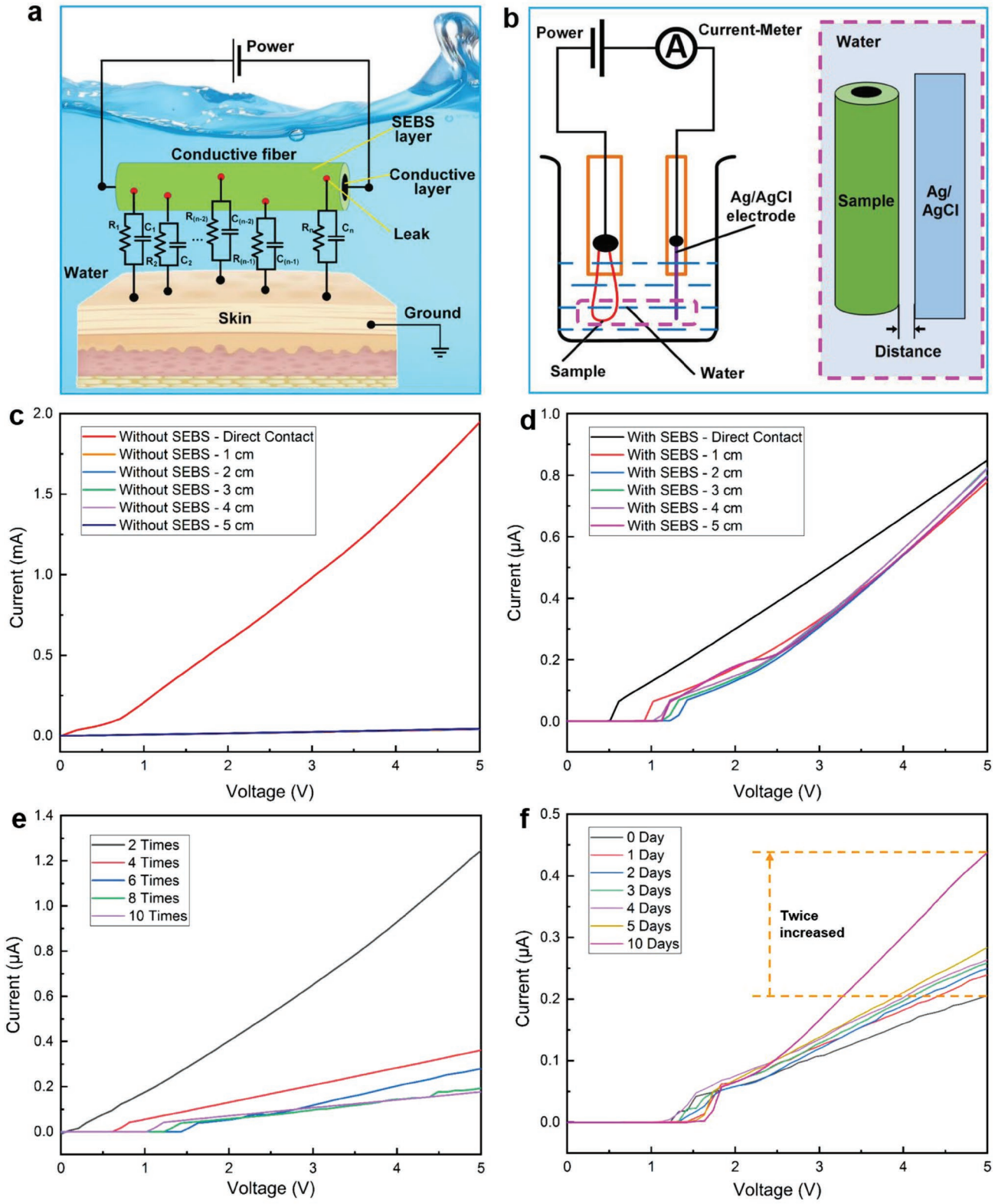

Figure 5. Conductivity–insulation effect of SEBS layer on CSCF. a) Circuit model of CSCF next to skin used in water. b) Experimental setup for testing the leakage current between CSCF and skin. Using Ag/AgCl as standard electrode to mimic skin, current between core–sheath fiber and Ag/AgCl was tested as leakage current sensed by skin. Applied voltage is set in the range of 0–5 V, as normally electronic device is driven below 5 V. c,d) Leakage current versus applied voltage of core–sheath fibers in same length c) without SEBS and d) with SEBS at different distances between fiber and Ag/AgCl electrode. e,f) Leakage current versus applied voltage of CSCFs in same length with various SEBS e) coating times and f) soaking time.

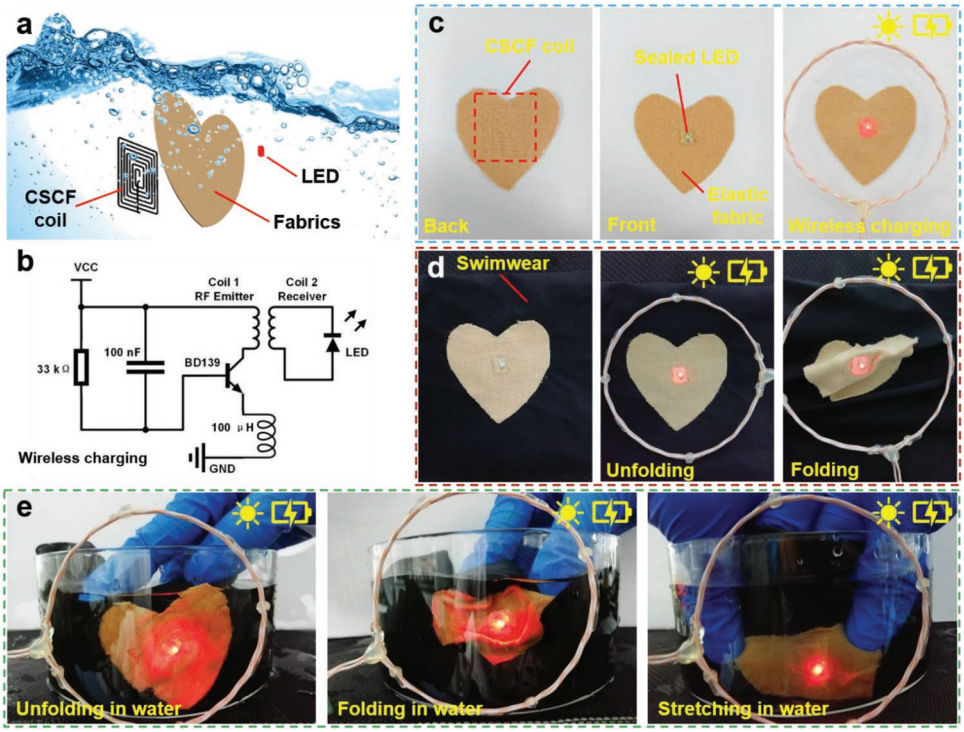

Figure 6. Application of CSCF as an induction coil used in underwater wireless charging patch for underwater wearable electronics. a) Schematic illustration of an underwater wireless charging patch. b) The circuit diagram for the wireless charging. c) Photos of wireless charging patches on elastic fabrics (kinesio tapes). Left: CSCF coil sewn in the back of an elastic fabric. Middle: A sealed LED fixed in front of an elastic fabric. Right: The patch lit an LED under a wireless charging emitter (circle). d) Photos of wireless charging patches on swimwear (Left) to light LEDs by wireless charging emitters. The patches are unfolding (Middle) and folding (Right). e) Photos of wireless charging patches to light LEDs in water under wireless charging. The patches are unfolding (Left), folding (Middle), and stretching (Right).

human can tolerate.[29] After fiber being coated with SEBS insulation layer (Figure 5d), when CSCF directly contacts with skin at applied voltage of 5 V, the maximum leakage current is less than 1 μA which is much lower than 0.5–1 mA, showing an almost three orders of magnitude decrease of that without SEBS layer. This indicates that SEBS layer could efficiently suppress leakage current to an extremely safe level (<1 μA at 5 V) when applying CSCF in underwater electronic skin devices.

SEBS thickness and time being used in water are two possible factors affecting insulation performance. Figure 5e compared the leakage current as a function of SEBS coating times. More coating times would lead to thicker SEBS layer and lower leakage current (details in Note S2 and Figure S7 in the Supporting Information). However, as shown in Figures S8 and S9 in the Supporting Information, the wrinkled surface featured in CSCF formed by buckling method will be weakened when SEBS coating time is more than four, resulting in a reduced electrical stability. To make CSCF as stretchable conductive fiber as well as being safe in water, SEBS layer of CSCF should be limited to a certain thickness (herein four spray coating times, ≈2 μm thickness each coating in radial direction). Also, capability of CSCF being long time used in water was evaluated (Figure 5f). When CSCF was continuously soaked in water as long as 10 days, the maximum leakage current at 5 V only increased by 2 times than that without water soaking. This suggests that with the protection of SEBS skin, our CSCF can continuously function in underwater electronic skin devices for quite a long time.

As a demonstration of CSCF functionally used in water for underwater wearable electronics (Figure S10, Supporting Information), an underwater wireless charging patch was fabricated and tested (**Figure 6**a,b). This patch consisted of three parts (Figure 6c): elastic fabric (kinesio tape) as a substrate, CSCF as an induction coil fixed at the back of an elastic fabric, and a red light emitting diode (LED) as charging output attached in front of elastic fabric. When a wireless charging emitter (details in Note S3 and Figure S11 in the Supporting Information) approached to the patch, LED would be lit via electromagnetic induction, indicating that CSCF is able to work as underwater inductance coil of wireless charging. Elastic swimwear can also be used as patch substrates. Figure 6d shows that the patches attached on black swimwear in both unfolding and folding shapes could light LEDs through wireless charging. This charging patch was then tested in water (Figure 6e), exhibiting consistently excellent performances no matter when the swimwear was unfolding, folding and stretching. This is one direct demonstration of core–sheath stretchable conductive fiber which is able to continuously work as wireless charging in underwater wearable electronics.

To summarize, a CSCF which could be safely used in water or other harsh environment (such as sonication) for a long time was presented. The ultrafine CSCF (≈30 μm in diameter) are composed of PU, MWCNTs, AgNWs, and SEBS orderly from

inside to outside. Spray coating 1D conductive networks onto a prestraining Lycra fiber resulted in a highly stretchable conductive fiber (e.g., $\Delta R/R_0 \approx 0.1$ at 100% strain, cycled > 100 000 times at 50% strain). Surface coating SEBS enabled a significantly reduced leakage both in current (<1 μA at 5 V, normalized) and materials, thus safe to human body (<0.5–1 mA). With this elastic and reliable protective SEBS skin, CSCF can be circled as a stretchable inductance coil and work as a wireless charging patch in water. This implies that our CSCF is promising as interconnector or electrode for underwater wearable electronics.

Experimental Section

Materials: Lycra fiber (main ingredient: polyurethane, specification: 10D) was purchased from Du Pont China Holding Co., Ltd. (Beijing, China). MWCNTs were obtained from Beifang Guoneng Technology Co., Ltd. (Beijing, China). AgNWs, (high aspect-ratio with the diameter of 70–100 nm and the length of 100–150 μm), were obtained from XFNANO (Nanjing, China). SEBS was purchased from Sigma-Aldrich, Co. (St. Louis, MO, USA). Ethanol (AR), toluene (AR) were purchased from Beijing Chemical Works (Beijing, China). Conductive silver paint (05001-AB) was sourced from SPI Supplies (West Chester, PA, USA).

Preparation of MWCNTs and AgNWs Dispersions and SEBS Solution: MWCNTs (25 mg) was dispersed in ethanol (10 mL) for 45 min using a probe sonicator (JY92-||N, 300 W, Ningbo Scientz Biotechnology Co., Ltd.) at 80% power. As-purchased AgNWs dispersion was 20 mg mL^{-1}. To adapt the spray-coating process, AgNWs was diluted to the concentration of 0.5 mg mL^{-1} using ethanol as dispersing solvent. 200 mg SEBS powder was fully dissolved in 20 mL toluene forming a clear solution.

Fabrication of CSCF: The fabrication process of CSCF was carried out in a fume hood at room temperature. Lycra fiber (PU) was cut into pieces accordingly. Those fiber pieces with same lengths were fixed on holders at initial spacing of 1 mm and then stretched up to 2–6 times of before stretching. Typical CSCF was being prestrained of 300%. After that, MWCNTs dispersion was spray coated around PU fibers by airbrush using compressed nitrogen at pressure of 30 psi. The outlet of airbrush kept a distance of approximately 10 cm with the surface of PU fiber. Before next coating, the chamber of airbrush was cleaned by ethanol, the solvent of MWCNTs dispersion. AgNWs dispersion and SEBS solution were spray coated as conductive layer and protective layer by airbrush in the same procedure. The parameter for SEBS spray coating was a little different at a larger working distance of ≈15 cm. After SEBS was fully cured, thus-fabricated fiber (PU@CNTs@AgNWs@SEBS) was released to free-stress status, forming wrinkles on its outer surface (Figures S2 and S12, Supporting Information). The density of MWCNTs and AgNWs, and thickness of SEBS around PU core were determined by spray-coating times. Without specification, all of those layers were spray coated four times in the typical CSCF (one reciprocating as one time).

Characterization: Morphology of CSCF was observed by Scanning Electron Microscope (SEM, SU8010, Hitachi), and its elements analysis was carried out by EDS (Esprit 2.0, Bruker Nano GmbH Berlin) equipped in SEM. The resistance of CSCF was measured by LCR meter (ECA200, Cycle-test). The leakage current was tested using digital source meter (Keithley 2636B) and Ag/AgCl as counter electrode (Lei-ci 218). Leakage element on cycling fatigue test was operated using digital control stretching stage (Custom-tailor, JiangYunGuangDian). The harsh water environment was mimicked in a water-bath sonicator at a power of 100% (KQ-300DE, 300 W, 40 KHz, Kunshan Ultrasonic Instrument Co., LTD).

Supporting Information

Supporting Information is available from the Wiley Online Library or from the author.

Acknowledgements

This work was supported by the Young Thousand Talents Program (110532103), the Beijing Normal University Startup funding (310421109, 312232102) and the Fundamental Research Funds for the Central Universities.

Conflict of Interest

The authors declare no conflict of interest.

Keywords

stretchable conductive fibers, underwater wearable electronics, underwater wireless charging

Received: October 4, 2019
Revised: November 5, 2019
Published online: December 1, 2019

[1] Y. J. Hong, H. Lee, J. Kim, M. Lee, H. J. Choi, T. Hyeon, D. H. Kim, *Adv. Funct. Mater.* **2018**, *28*, 1805754.
[2] W. Gao, S. Emaminejad, H. Y. Y. Nyein, S. Challa, K. Chen, A. Peck, H. M. Fahad, H. Ota, H. Shiraki, D. Kiriya, D. H. Lien, G. A. Brooks, R. W. Davis, A. Javey, *Nature* **2016**, *529*, 16521.
[3] C. Wang, C. Wang, Z. Huang, S. Xu, *Adv. Mater.* **2018**, *30*, 1801368.
[4] J. Xu, S. Wang, G. N. Wang, C. Zhu, S. Luo, L. Jin, X. Gu, S. Chen, V. R. Feig, J. W. F. To, S. Rondeau-Gagne, J. Park, B. C. Schroeder, C. Lu, J. Y. Oh, Y. Wang, Y. Kim, H. Yan, R. Sinclair, D. Zhou, G. Xue, B. Murmann, C. Linder, W. Cai, J. B. H. Yok, J. W. Chung, Z. Bao, *Science* **2017**, *355*, 59.
[5] S. Choi, S. I. Han, D. Jung, H. J. Hwang, C. Lim, S. Bae, O. K. Park, C. M. Tschabrunn, M. Lee, S. Y. Bae, J. W. Yu, J. H. Ryu, S. Lee, K. Park, P. M. Kang, W. B. Lee, R. Nezafat, T. Hyeon, D. Kim, *Nat. Nanotechnol.* **2018**, *13*, 1048.
[6] T. Cheng, Y. Zhang, W. Lai, W. Huang, *Adv. Mater.* **2015**, *27*, 3349.
[7] H. Wang, M. He, Y. Zhang, *Acta Phys.-Chim. Sin.* **2019**, *35*, 1207.
[8] N. Matsuhisa, M. Kaltenbrunner, T. Yokota, H. Jinno, K. Kuribara, T. Sekitani, T. Someya, *Nat. Commun.* **2015**, *6*, 7461.
[9] C. Wang, K. Xia, H. Wang, X. Liang, Z. Yin, Y. Zhang, *Adv. Mater.* **2019**, *31*, 1801072.
[10] W. Zeng, L. Shu, Q. Li, S. Chen, F. Wang, X. M. Tao, *Adv. Mater.* **2014**, *26*, 5310.
[11] S. Lee, S. Shin, S. Lee, J. Seo, J. Lee, S. Son, H. J. Cho, H. Algadi, S. Al-Sayari, D. E. Kim, T. Lee, *Adv. Funct. Mater.* **2015**, *25*, 3114.
[12] Y. Huang, H. Hu, Y. Huang, M. Zhu, W. Meng, C. Liu, Z. Pei, C. Hao, Z. Wang, C. Zhi, *ACS Nano* **2015**, *9*, 4766.
[13] K. Dong, Z. Wu, J. Deng, A. C. Wang, H. Zou, C. Chen, D. Hu, B. Gu, B. Sun, Z. L. Wang, *Adv. Mater.* **2018**, *30*, 1804944.
[14] Z. F. Liu, S. Fang, F. A. Moura, J. N. Ding, N. Jiang, J. Di, M. Zhang, X. Lepró, D. S. Galvão, C. S. Haines, N. Y. Yuan, S. G. Yin, D. W. Lee, R. Wang, H. Y. Wang, W. Lv, C. Dong, R. C. Zhang, M. J. Chen, Q. Yin, Y. T. Chong, R. Zhang, X. Wang, M. D. Lima, R. Ovalle-Robles, D. Qian, H. Lu, R. H. Baughman, *Science* **2015**, *349*, 6246.
[15] R. Ma, J. Lee, D. Choi, H. Moon, S. Baik, *Nano Lett.* **2014**, *14*, 1944.
[16] P. Chen, Y. Xu, S. He, X. Sun, W. Guo, Z. Zhang, L. Qiu, J. Li, D. Chen, H. Peng, *Adv. Mater.* **2015**, *27*, 1042.
[17] R. Cruz-Silva, A. Morelos-Gomez, H. Kim, H. Jang, F. Tristan, S. Vega-Diaz, L. P. Rajukumar, A. L. Elias, N. Perea-Lopez, J. Suhr, M. Endo, M. Terrones, *ACS Nano* **2014**, *8*, 5959.

[18] J. Lee, H. Kwon, J. Seo, S. Shin, J. H. Koo, C. Pang, S. Son, J. H. Kim, Y. H. Jang, D. E. Kim, T. Lee, *Adv. Mater.* **2015**, *27*, 2433.
[19] Y. Shang, Y. Li, X. He, L. Zhang, Z. Li, P. Li, E. Shi, S. Wu, A. Cao, *Nanoscale* **2013**, *5*, 2403.
[20] P. L. Floch, X. Yao, Q. Liu, Z. Wang, G. Nian, Y. Sun, L. Jia, Z. Suo, *ACS Appl. Mater. Interfaces* **2017**, *9*, 25542.
[21] L. Yu, J. C. Yeo, R. H. Soon, T. Yeo, H. H. Lee, C. T. Lim, *ACS Appl. Mater. Interfaces* **2018**, *10*, 12773.
[22] M. A. H. Khondoker, A. Ostashek, D. Sameoto, *Adv. Eng. Mater.* **2019**, *21*, 1900060.
[23] S. Wang, N. Liu, J. Su, L. Li, F. Long, Z. Zou, X. Jiang, Y. Gao, *ACS Nano* **2017**, *11*, 2066.
[24] X. Zhong, Y. Li, Y. Liu, X. Qiao, Y. Feng, J. Liang, J. Jin, L. Zhu, F. Hou, J. Li, *Adv. Mater.* **2010**, *22*, 692.
[25] Z. Liu, D. Qi, G. Hu, H. Wang, Y. Jiang, C. Chen, Y. Luo, X. J. Loh, B. Liedberg, X. Chen, *Adv. Mater.* **2018**, *30*, 1704229.
[26] Z. Pei, Y. Zhang, G. Chen, *Text. Res. J.* **2019**, *89*, 113.
[27] B. Choi, J. Lee, H. Han, J. Woo, K. Park, J. Seo, T. Lee, *ACS Appl. Mater. Interfaces* **2018**, *10*, 36094.
[28] Z. Yin, M. Jian, C. Wang, K. Xia, Z. Liu, Q. Wang, M. Zhang, H. Wang, X. Liang, X. Liang, Y. Long, X. Yu, Y. Zhang, *Nano Lett.* **2018**, *18*, 7085.
[29] Eisner Safety Consultants is Proud to Present a Series on IEC 60601-1, http://www.eisnersafety.com/downloads/Leakage_Part1.pdf (accessed: March 2019).
[30] Z. Wang, Y. Huang, J. Sun, Y. Huang, H. Hu, R. Jiang, W. Gai, G. Li, C. Zhi, *ACS Appl. Mater. Interfaces* **2016**, *8*, 24837.
[31] Y. Cheng, R. Wang, J. Sun, L. Gao, *Adv. Mater.* **2015**, *27*, 7365.
[32] N. Bowden, S. Brittain, A. G. Evans, J. W. Hutchinson, G. M. Whitesides, *Nature* **1998**, *393*, 146.
[33] J. A. Rogers, T. Someya, Y. Huang, *Science* **2010**, *327*, 1603.
[34] B. Zhang, J. Lei, D. Qi, Z. Liu, Y. Wang, G. Xiao, J. Wu, W. Zhang, F. Huo, X. Chen, *Adv. Funct. Mater.* **2018**, *28*, 1801683.
[35] H. Liu, H. Hsieh, J. Chen, C. Shih, W. Lee, Y. Chiang, W. Chen, *Macromol. Chem. Phys.* **2019**, *220*, 1800387.
[36] S. Duan, Z. Wang, L. Zhang, J. Liu, C. Li, *ACS Appl. Mater. Interfaces* **2017**, *9*, 30772.
[37] D. J. Lipomi, M. Vosgueritchian, B. C. Tee, S. L. Hellstrom, J. A. Lee, C. H. Fox, Z. Bao, *Nat. Nanotechnol.* **2011**, *6*, 788.
[38] L. Jin, A. Chortos, F. Lian, E. Pop, C. Linder, Z. Bao, W. Cai, *Proc. Natl. Acad. Sci. USA* **2018**, *115*, 1986.
[39] M. Su, Z. Huang, F. Li, Z. Zhang, Y. Guo, Z. Cai, Y. Li, W. Li, X. Qian, Y. Li, X. Zhang, Y. Song, *Adv. Mater. Technol.* **2018**, *3*, 1800107.
[40] Products, http://generalpolymers.net/sebs.cfm (accessed: March 2019).
[41] D. Son, Z. Bao, *ACS Nano* **2018**, *12*, 11731.
[42] N. Matsuhisa, D. Inoue, P. Zalar, H. Jin, Y. Matsuba, A. Itoh, T. Yokota, D. Hashizume, T. Someya, *Nat. Mater.* **2017**, *16*, 834.
[43] W. Lee, D. Kim, N. Matsuhisa, M. Nagase, M. Sekino, G. G. Malliaras, T. Y. T. Someya, *Proc. Natl. Acad. Sci. USA* **2017**, *114*, 10554.
[44] H. Fang, J. Zhao, K. J. Yu, E. Song, A. B. Farimani, C. Chiang, X. J. Y. Xue, D. Xu, W. Du, K. J. Seo, Y. Zhong, Z. Yang, S. M. Won, G. Fang, S. W. Choi, S. Chaudhuri, Y. Huang, M. A. Alam, J. Viventi, N. R. Aluru, J. A. Rogers, *Proc. Natl. Acad. Sci. USA* **2016**, *113*, 11682.

